Journal of Peptide Science
J. Peptide Sci. 2006; **12**: 180–189
Published online 22 August 2005 in Wiley InterScience (www.interscience.wiley.com). DOI: 10.1002/psc.714

JOURNAL OF PEPTIDE SCIENCE

Analysis of interactions responsible for vasopressin binding to human neurohypophyseal hormone receptors – molecular dynamics study of the activated receptor–vasopressin–G_α systems

MAGDALENA J. ŚLUSARZ,* ARTUR GIEŁDOŃ, RAFAŁ ŚLUSARZ and JERZY CIARKOWSKI

Faculty of Chemistry, University of Gdańsk, Sobieskiego 18, 80-952 Gdańsk, Poland

Received 5 April 2005; *Revised 14 June 2005*; *Accepted 28 June 2005*

Abstract: Vasopressin (CYFQNCPRG-NH_2, AVP) is a semicyclic endogenous peptide, which exerts a variety of biological effects in mammals. The main physiological roles of AVP are the regulation of water balance and the control of blood pressure and adrenocorticotropin hormone (ACTH) secretion, mediated via three different subtypes of vasopressin receptors: V1a, V1b and V2 receptors (V1aR, V1bR and V2R, respectively). They are the members of the class A, G-protein-coupled receptors (GPCRs). AVP also modulates several behavioral and social functions. In this study, the interactions responsible for AVP binding to vasopressin V1a and V2 receptors *versus* the closely related oxytocin ([I3,L8]AVP, OT) receptor (OTR) have been investigated. Three-dimensional models of the activated receptors were constructed using multiple sequence alignment, followed by homology modeling using the complex of activated rhodopsin with Gt_α *C*-terminal peptide of transducin MII-Gt(338-350) prototype as a template. AVP was docked into the receptor-G_α systems. The three lowest-energy pairs of receptor-AVP-G_α (two complexes per each receptor) were selected. The 1-ns unconstrained molecular dynamics (MD) of complexes embedded into the fully hydrated 1-palmitoyl-2-oleoyl-*sn*-glycero-3-phosphatidylcholine (POPC) lipid bilayer was conducted in the AMBER 7.0 force field. Six relaxed receptor-AVP-G_α models were obtained. The residues responsible for AVP binding to vasopressin receptors have been identified and a different mechanism of AVP binding to V2R than to V1aR has been proposed. Copyright © 2005 European Peptide Society and John Wiley & Sons, Ltd.

Keywords: AVP; GPCR activation; molecular dynamics; phospholipid bilayer; vasopressin

INTRODUCTION

The vasopressin V1a, V1b and V2 receptors (V1aR, V1bR and V2R, respectively) belong to the class A, G-protein-coupled receptors (GPCRs) and mediate the cellular actions of the neurohypophyseal hormones: arginine vasopressin (CYFQNCPRG–NH_2, AVP) and to a lower degree, oxytocin ([I3,L8]AVP, OT) [1–4]. V1aR, V1bR and V2R along with the OT receptor (OTR) constitute the neurohypophyseal hormone receptors subgroup of class A [1]. The neurohypophyseal hormone receptors share a high degree (35–50%) of sequence identity (Figure 1) and exhibit certain conserved sequence motifs [5]. Accordingly, they display related pharmacological profiles [6], which is in accord with the similarity of chemical structure of their endogenous ligands AVP and OT. On a molecular level, both hormones are nonapeptides with a disulfide bridge, which results in a 20-membered *N*-terminal tocin ring Cys1–Cys6 and a *C*-terminal α–amidated linear tripeptidic tail. Their peptide sequences differ only in the amino acids at positions 3 and 8. Arg8 is crucial for interaction with vasopressin receptors, while Ile3 for stimulation of OTR [7]. The difference in the polarity of amino acids in these positions is critical for selectivity and interaction with the respective receptors [1]. In Table 1, experimental affinities of AVP and OT toward the respective receptors are specified [8]. V1aR, located in the vascular smooth muscle are responsible mainly for increase of blood pressure and mediation of remaining physiological functions of AVP [9,10], with the exception of those mediated *via* V1bR and V2R. The latter is found in the collecting duct (CD) of the kidney, where it mediates the antidiuretic effect of vasopressin: water reabsorption and concentration of the urine [11,12]. The V1b (also termed V3) pituitary receptor, not a subject of this work, controls adrenocorticotropin hormone (ACTH) secretion and AVP actions in the central nervous system [13,14]. OTR is involved mainly in the control of labor and lactation [15–17].

Abbreviations: AVP, arginine vasopressin, vasopressin; CSA, constrained simulated annealing; EL, extracellular loop; G-protein, guanine nucleotide-binding protein; GPCR, G-protein-coupled receptor; Gq/11, G-protein class interacting with phospholipase C; Gs, G-protein class interacting with adenylyl cyclase; IL, intracellular loop; MD, molecular dynamics; MII, Meta II, activated form of rhodopsin, OT, oxytocin; OTR, oxytocin receptor; PME, particle-mesh Ewald; POPC, 1-palmitoyl-2-oleoyl-*sn*-glycero-3-phosphatidylcholine; RD, rhodopsin; RMSd, root mean square deviation; TM, transmembrane α-helix; V1aR, vasopressin V1a receptor; V2R, vasopressin V2 receptor; 7TM, heptahelical transmembrane domain.

*Correspondence to: M. J. Ślusarz, Faculty of Chemistry, University of Gdańsk, Sobieskiego 18, 80-952 Gdańsk, Poland;
e-mail: magda@chem.univ.gda.pl

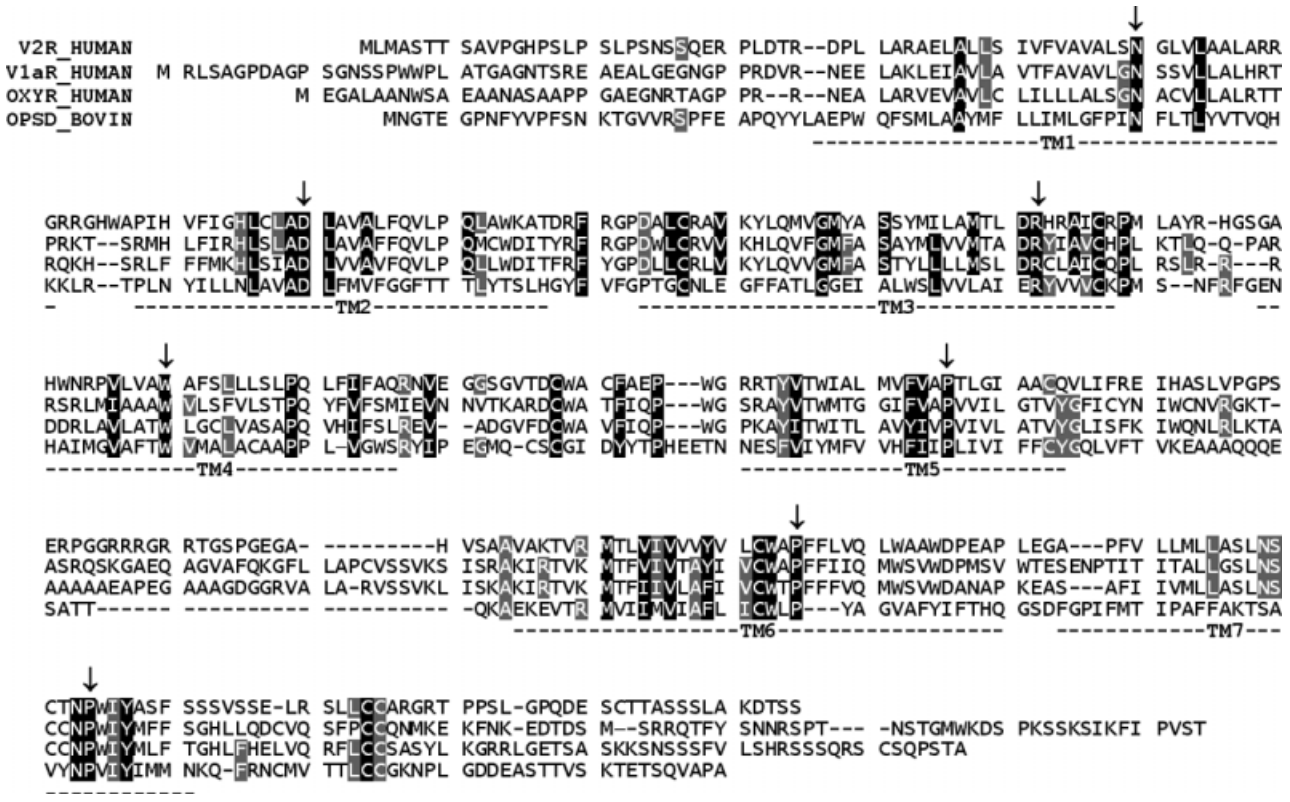

Figure 1 Primary sequence alignment of the human neurohypophyseal hormone receptors (OTR, V1aR and V2R), and bovine rhodopsin, done using the Multalin program [19]. The putative transmembrane helices 1–7 are underlined. The conservative residues, indicative of high-level similarity within the subfamily, are shown in black while those with lower-level similarity are shown in gray [17]. The 'N'50 residues are marked with an arrow [20].

Table 1 Experimental affinities of AVP and OT toward respective receptors. The affinity values are given in the IU/mg [8]

	V2R	V1aR	OTR
AVP	465	412	17
OT	5	5	450

Furthermore, interacting with the respective receptors, both AVP and OT play a role in many reproductive, behavioral and social functions [18].

Neurohypophyseal hormone receptors, being typical members of class A GPCR, are membrane-spanning proteins consisting of seven transmembrane helices (TM1–TM7), connected by alternating extracellular (EL) and intracellular (IL) loops. Their sequences begin with extracellular *N*-terminus and end with the cytosolic *C*-terminus [21–23]. The crystal structure of the most studied class A member, the inactive bovine rhodopsin ('dark' rhodopsin, RD) was published in 2000 [21], providing the first structure of a GPCR at atomic resolution. It is an agreement in regard to 3D-structural homology within heptahelical transmembrane domain (7TM) among Class A of GPCR, thus RD makes a good structural template for other family members [23–28]. GPCRs are functionally coupled to heterotrimeric G-proteins (guanine nucleotide-binding protein) composed of three subunits, termed α, β and γ and being classified into four families: Gs, Gi, Gq and G12 [29,30]. V1aR, V1bR and OTR are linked to Gq/11 protein that stimulates the activity of phospholipase C, whereas V2R is coupled to the Gs protein that stimulates adenylyl cyclase [1,2]. On the molecular level, if the agonist binds to a GPCR, the receptor gets activated by undergoing an allosteric rearrangement that allows an accommodation of interacting fragments of a cytosolic G-protein at the receptor–G-protein interface. GPCRs are targets of more than 50% of all therapeutically used drugs. Hence, understanding how the interaction with agonist differs from that with antagonist and identification of GPCR activation mechanism are fundamental problems in the rational drug design [24,31–33]. It has been known that vasopressin receptors are involved in a number of pathological conditions, thus the ligands capable of selective stimulation or blockade of the respective vasopressin receptors may present therapeutic benefit in a variety of diseases [34–38]. Unfortunately, the molecular mechanism of GPCR activation is still unknown, although some of its aspects are generally accepted. In

the case of RD, it is known that activation involves a movement of the TM6, TM7 and TM2 cytosolic halves, with accompanying loop fragments, outside of the 7TM bundle [39,40]. This dislocation of the cytosolic side of TM6 is in addition accompanied by its clockwise (when viewed from the cytosol) rotation [39]. These conformational rearrangements eventually result in conversion from rhodopsin to *meta* rhodopsin (Meta II, MII). It is also known that the *C*-terminal peptides Gt_α(340–350) [41,42] and Gt_γ(60–72)farnesyl [43] of transducin α and γ segments, respectively, independently stabilize Meta II [44–46]. Gt_α(340–350) makes an α-helical extension of the last α5 Gt_α helix, potentially fitting into the MII cavity on its cytosolic side [47–49]. Thus it was proposed that in any class A receptor–G-protein system, an agonist-induced rearrangement takes place, involving conservative residues of both parts in a set of consensus interactions [49]. Accordingly, the low-resolution model of the MII monomer docking Gt_α(338–350) was used in our former study [50] as the template for construction of three-dimensional models of activated models of V2R, V1aR and OTR complexing suitable interacting G_α fragments. The equivalent receptor–G_α-segment models are used in the present work for AVP docking, subsequent molecular dynamics (MD) simulation in 1-palmitoyl-2-oleoyl-*sn*-glycero-3-phosphatidylcholine (POPC) bilayer and identification of the putative AVP binding sites.

METHODS

Parameterization and Model Building

Nonstandard amino acid residues and other structure fragments were parameterized as recommended in the AMBER 7.0 manual [51]. Specifically, the point atom charges were fitted by applying the RESP procedure [52,53] to the electrostatic potential calculated in the 6–31 G* basis set using the program GAMESS98 [54]. The three-dimensional model of AVP was constructed via homology modeling, using the coordinates of pressinoic acid [55] and the BIOPOLYMER module of SYBYL package [56]. The three-dimensional models of activated neurohypophyseal hormone receptors (V2R, V1aR and OTR) and the *C*-terminal fragments of suitable G_α necessary to keep the receptor in activated state were constructed as described previously [50], using the model of MII–Gt_α(338–350), being the appropriate modification of the X-ray RD structure [49] as a template.

Docking and MD Simulation

AVP was docked to the V2R–Gs(382–394), V1aR–Gq/11 (347–359) and OTR–Gq/11(347–359) systems, using a modified genetic algorithm as implemented in the program AUTODOCK [57,58], for details see [59–61]. The constrained simulated annealing (CSA) protocol *in vacuo* for 15 ps [62,63] and energy minimization with positional constrains on C^α atoms in 7TM to retain the receptors shape in homology to MII, were done. Two lowest-energy systems per each receptor–ligand–G_α-segment were chosen and consequently six selected complexes were inserted into the fully hydrated POPC bilayer model [64,65] and submitted to the MD simulation, carried out in AMBER 7.0 force field [51], following the same conditions (periodic box components) as described previously [50]. MD was performed using the particle-mesh Ewald (PME) electrostatic summation [66–68] and the OPLS united atom parameters were applied for all components of the each receptor–ligand–G_α-segment system [69]. The flat-bottom soft harmonic-wall restraints were imposed onto the φ, ψ and ω peptide angles of the 7TM amino acid residues to avoid unfolding or any other unwanted modifications of the TM helices. In accordance with the former AMBER protocol [50], the positional TM C^α constraints were used exclusively for the first 100 ps of the simulation during heating the system from 0 to 300 K, to prevent the helices from perturbation. From 100 ps to 1000 ps, free MD simulation without positional constraints was carried out. In the final step, the energy minimization of the 1-ns MD snapshots in AMBER 7.0 [51], was done.

Residue Indexing

For the convenience of reading, the AVP residues are identified using three letter codes with the indices in parentheses, e.g. Phe(3), while the receptors residues are identified using one letter codes with the universal class A indices (Ballesteros–Weinstein numbering scheme [20]) placed as superscripts, followed by the absolute numbers, e.g. V2R $Q^{4.66}$180 or by absolute numbers of respective (V2R, V1aR, OTR) receptor residues e.g. $W^{6.48}$(284, 304, 288) describing the interactions of conservative residues. Briefly, in the Ballesteros–Weinstein scheme, the specific residue number defines a position relative to the most conserved residue in the TM helix 'N', which is assigned the number 'N'50. For example, $Q^{4.66}$180 indicates a residue in TM4, located 16 residues to $W^{4.50}$164, which is the most conserved residue in TM4. Residues placed in loops are identified with one letter code, followed only by the residue absolute number, e.g. EL2 E198.

Abbreviations of the Complexes Names

In the Results section describing receptor–ligand interactions, in the three-component names of complexes, e.g. 'the receptor–AVP–G_α-segment', the clause 'G_α-segment' will be omitted for better legibility of the text.

RESULTS AND DISCUSSION

Analysis of Receptor–AVP Interactions

After MD simulation, six relaxed receptor–AVP complexes have been obtained. One complex per each receptor, that of lower energy in any pair, was finally selected for further detailed examination. The receptor amino acid residues comprising the putative AVP binding pocket were selected using the distance criterion, according to which receptor residues any atom of which was not farther than 3.5 Å from any atom of AVP residues were tentatively selected. Subsequently, all receptor residues not involved in any interaction were

Table 2 List of the V2R, V1aR and OTR residues, involved in the interactions with AVP

TM 'N'domain	V2R	V1aR	OTR	Universal numbering[a]
TM1	—	E54	E42	1.35
TM2	V88	V100	V88	2.53
	Q92	Q104	Q92	2.57
	Q96	Q108	Q96	2.61
TM3	—	V127	—	3.28
	Q119	Q131	Q119	3.32
	M120	V132	V120	3.33
	M123	M135	M123	3.36
	Y124	—	F124	3.37
	S127	—	T127	3.40
TM4	Q174	Q185	Q171	4.60
	Q180	—	—	4.66
TM5	R202	—	—	5.35
	—	—	I201	5.39
	I209	—	I204	5.42
	—	I224	—	5.46
	F214	F225	Y209	5.47
TM6	W284	W304	—	6.48
	F287	F307	F291	6.51
	Q291	Q311	Q295	6.55
TM7	F307	I330	F311	7.35
	—	T333	V314	7.38
	M311	A334	M315	7.39
	—	—	A318	7.42
	—	—	S319	7.43
	N317	N340	—	7.45
EL2	R181	I192	—	
	—	N196	—	
	—	T198	—	
	—	K199	—	
	T190	R201	F185	
	D191	—	W188	
	—	—	—	
	E198	—	—	

[a] Ref. 20.

omitted after visual inspection. The remaining residues were proposed as interacting with AVP (Table 2 and Figure 2).

Changes in the Receptor Structures During Molecular Dynamics

All receptor-AVP complexes remained stable during 1-ns unconstrained MD simulation, and there were no significant conformational changes of the receptor structures. The root mean square deviations (RMSd) measured on the all atoms/C^{α} atoms of the 7TM were: 2.64 Å/2.04 Å for V2R, 2.56 Å/1.71 Å for V1aR and 3.04 Å/2.37 Å for OTR. The RMSd changes during MD are presented in Figure 3. The higher RMSd for OTR might result from fewer than V2R or V1aR strong receptor–ligand interactions contributing to the stability of the receptor–ligand complex. Conversely, the higher RMSd for V2R during the MD simulation with OT was observed in our former work [50].

Ligand Location and Conformation Inside the Binding Pockets

AVP binding pockets are formed mainly within TM2–TM7, except the only TM1 residue $E^{1.35}$ (–, 54, 42) interacting with the ligand in V1aR and OTR (see the following text). The location of AVP is vertical (parallel to the longer axis of the receptor) in V2R and V1aR contrary to the location in OTR, where the ligand position is rather horizontal (perpendicular to the longer axis of the receptor), (Figure 2). It is remarkable that the 'horizontal' OT location in the same receptors has been observed, as described in our former work [50]. Correspondingly, the conformation of AVP molecule is different in each receptor, as one may see in Figure 4, where the superposition of AVP structures before and after MD is presented. The location of AVP in all receptors did not change significantly during MD, nor did the conformation of its side chains; thus RMSd measured on the all atoms/C^{α} atoms of AVP were: 1.67 Å/0.57 Å in V2R, 1.51 Å/0.64 Å in V1R and 1.445 Å/0.54 Å in OTR. In V2R, two aromatic rings of AVP Tyr(2) and Phe(3) are exactly parallel and may interact strongly with each other. It is noticeable that this orientation resulted only from unconstrained MD simulation, reflecting relaxation and better-fitting ligand into the receptor cavity. Both Tyr(2) and Phe(3) are situated on the edge of the ligand outside the macrocyclic ring, whereas in V1aR the Phe(3), dislocation over the tocin ring toward disulfide bridge results in reduction of an aromatic interaction with Tyr(2). However, in this complex also, both aromatic rings are located more parallel in AVP conformation after MD. It has been proposed that orientation of the Tyr(2) side chain determines neurohypophyseal hormone receptors activation and signal transduction [70], therefore parallel Phe(3) to Tyr(2) orientation as described may in addition stabilize extended location of the latter in V2R. Furthermore, the stability for AVP conformation in V2R is provided via two hydrogen bonds between peptide backbone as in the crystal structure of deamino-oxytocin, where the same β-turn is formed [71]. Therefore, Asn(5) carbonyl oxygen and amide proton interacts with the Tyr(2) amide proton and carbonyl oxygen, respectively. In V1aR the γ-turn is formed, and stabilization results from hydrogen bonds formed by Gln(4) amide proton and Tyr(2) carbonyl oxygen. Moreover, in V2R side chain, amide proton of Gln(4) is involved in a hydrogen bond with Cys(1) carbonyl oxygen, while the main chain Gln(4) carbonyl oxygen interacts with Cys(1) amino group in the V1aR. For this reason, in V2R the carboxamide of the Gln(4) is

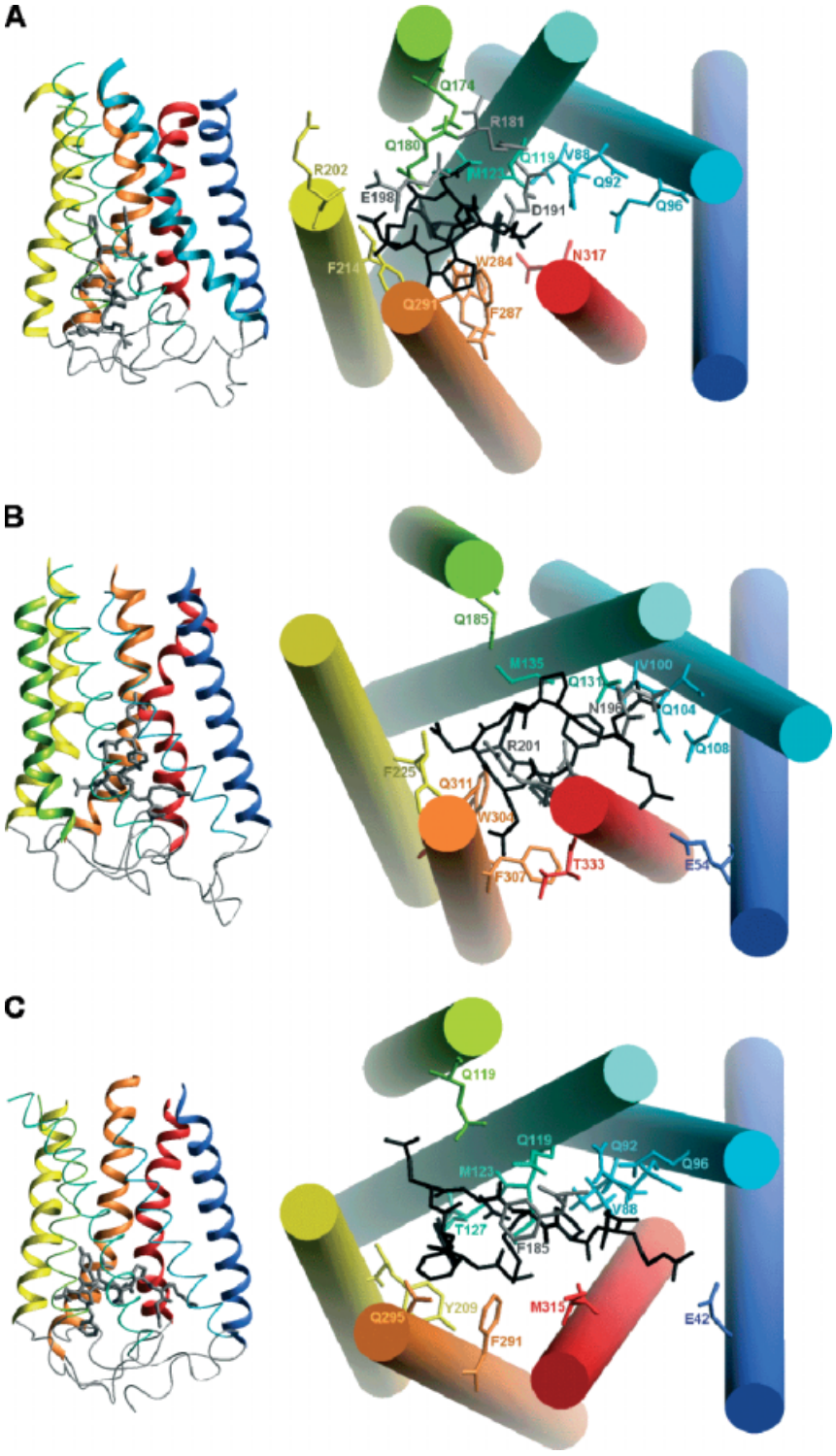

Figure 2 Representation of the AVP binding pocket in neurohypophyseal hormone receptors. Panel A – V2R, Panel B – V1aR, Panel C – OTR. The TM helices are colored from blue (TM1) to red (TM7). On the left, the location of ligand inside the binding cavities is shown. The several helices are made thinner and the intracellular loops omitted for clarity. On the right, the binding amino acid residues are marked and their side chains exposed, they are colored in harmony with TM colors, while the EL2 residues are gray.

folded back over the ring moiety in an opposite way to its location in V1aR, where it is extended away from the macrocyclic ring and strongly exposed for interactions with the receptor. In both AVP conformations, in V2R and V1aR, Asn(5) not involved in any intramolecular hydrogen bonds are accessible for interaction with the receptor, more in V1aR than in V2R, where the Asn(5) side chain is slightly bent toward the macrocyclic ring.

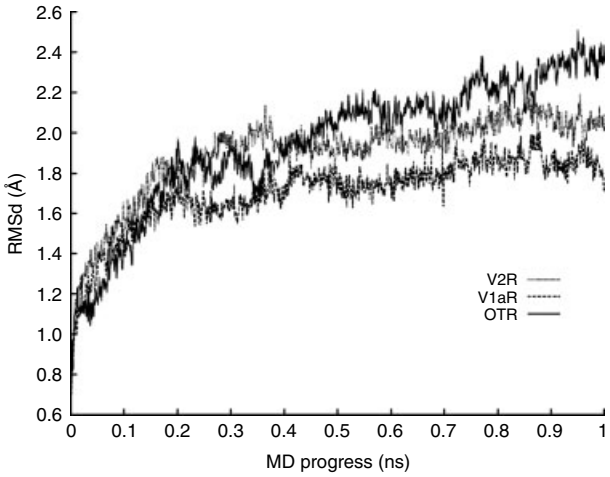

Figure 3 Representation of the RMSd changes observed during MD. For details, see the *Results* section.

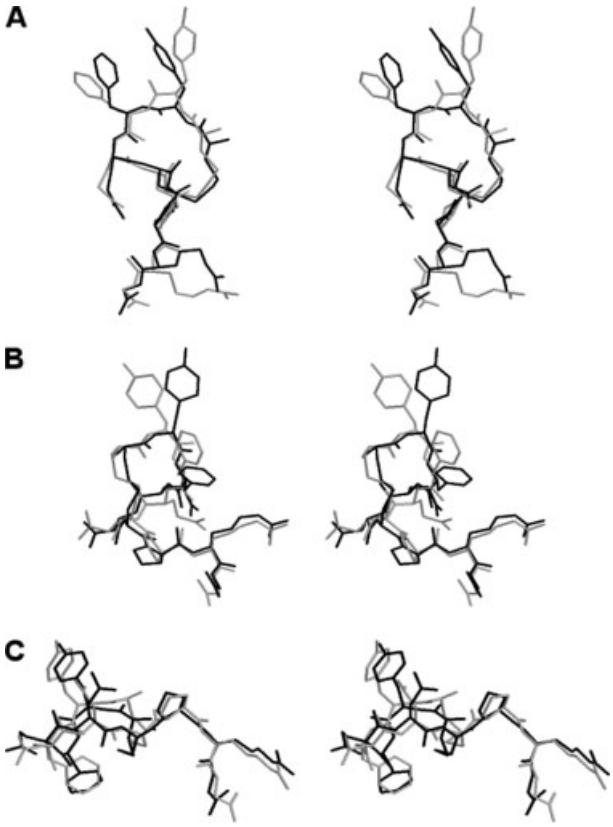

Figure 4 Stereodiagrams of superimposition of the AVP conformations inside the respective receptors before (gray) and after (black) MD. Panel A – V2R; Panel B – V1aR; Panel C – OTR.

AVP conformation in OTR differs from those in V2R and V1aR. The macrocyclic ring is stabilized by several hydrogen bonds; thus amide proton and carbonyl oxygen of Cys(6) form hydrogen bonds with the carbonyl oxygen and the *N*-terminal amine proton of Cys(1), respectively, and the carbonyl oxygen of Phe(3) is involved in a hydrogen bond with the amide proton of Asn(5). The major difference is found in the orientation of aromatic side chains of the Tyr(2) and Phe(3). They are both perpendicular to the plane of the macrocyclic ring and situated on the opposite sides of the latter. Thus, there is no chance for a stacking interaction (see earlier section) that might stabilize the orientation of Tyr(2) side chain, typical of active complex. Moreover, hydrogen bonding between Tyr(2) hydroxyl and Asn(5) carboxamide proton has been observed. In addition, Asn(5) carboxamide location is stabilized via another hydrogen bond formed with the amide proton of Cys(6). As a result, the Asn(5) carboxamide is less accessible for interacting with receptor, in contrast to full accessible carboxamide of Gln(4). Furthermore, in all three complexes, AVP Arg(8) and $GlyNH_2$(9) side chains are not involved in any intramolecular hydrogen bonds, thus they are well exposed and may interact with the receptor cavity residues. Described differences in the AVP conformation inside the vasopressin receptors *versus* OTR, especially location of side chains crucial for interaction with the receptors, might help explain significant differences in receptor–ligand affinities (see Table 1).

Highly Conserved 7TM Residues Stabilize Activated Receptor–AVP Complexes

All three receptor–ligand complexes are stabilized by networks of interactions involving the highly conserved Gln residues (for all interactions see Figure 3 and Table 2): $Q^{2.57}$(92, 104, 92); $Q^{2.61}$(96, 108, 96); $Q^{3.32}$(119, 131, 119); $Q^{4.60}$(174, 185, 171), $Q^{6.55}$(291, 311, 295) appearing to be most important anchors keeping the ligand inside the binding site. In the V2R–AVP complex, as many as three conserved Gln residues: $Q^{3.32}$119, $Q^{4.60}$174 and $Q^{6.55}$291 form hydrogen bonds with the AVP Asn(5) simultaneously, hence they seem to be especially important for AVP binding. Thus, the $Q^{3.32}$119 and $Q^{4.60}$174 carboxamides interact with the carboxamide of Asn(5). Another hydrogen bond is observed between the carboxamide of $Q^{6.55}$291 and the main chain carbonyl of Asn(5). Moreover, the $Q^{6.55}$291 carboxamide interacts also with the Phe(3) main chain carbonyl. The remaining conserved $Q^{2.57}$92 and $Q^{2.61}$96 are also involved in hydrogen bonding via their carboxamides and interact with the *N*-terminal amino group of Cys(1). However, these interactions do not appear to be crucial for binding, since it has been confirmed that the *N*-terminal amine is not required for agonist binding [72,73]. In the V1aR–AVP complex, hydrogen bonds involving $Q^{3.32}$131 and $Q^{6.55}$311 are formed between the carboxamides of the latter and the main chain carbonyl of Pro(7) and amide proton of Asn(5), respectively. However, the most important interaction is a strong hydrogen bond formed by the carboxamide

of $Q^{2.61}$108 and positively charged guanidino group of Arg(8). Similar interaction is also observed in the OTR–AVP complex, where two conserved Gln residues $Q^{2.57}$92 and $Q^{2.61}$96 interact with the same Arg(8) guanidino group via their carboxamides. Furthermore, in this complex also two hydrogen bonds have been observed: that between the $Q^{3.32}$119 carboxamide and the main chain carbonyl of Asn(5), and between the $Q^{4.60}$171 and Gln(4) carboxamides. Described interactions involving conserved Gln residues appear to be crucial to stabilize the activated receptor–agonist complexes. It is remarkable that exactly the same residues were identified by mutagenesis studies as responsible for binding neurohypophyseal hormones and their analogs to rat vasopressin V1a receptor [74]. Moreover, possible contribution of highly conserved Gln residues for binding of OT to human neurohypophyseal hormone receptors was proposed in our former study [50]. Besides Gln residues, in all three complexes, three other conservative residues: $V^{2.53}$(88, 100, 88), $M^{3.36}$(123, 135, 123) and $F^{6.51}$(287, 307, 291) seem to be more weakly involved in stabilization of the receptor–ligand complexes, similar to $W^{6.48}$(284, 304, –) appearing exclusively in the complexes with vasopressin receptors.

Furthermore, one more conserved residue $N^{7.45}$(317, 340, –) interacts with AVP only in V2R and V1aR. In both complexes, the carboxamide of $N^{7.45}$(317, 340, –) forms a hydrogen bond with the hydroxyl of Tyr(2) and this strong interaction does not occur in the OTR–AVP complex, as a result of dissimilar AVP location. It is possible that the described interaction might play a significant role in the receptor activation and in stabilization of the complex with an agonist. It has been experimentally demonstrated that the deletion or substitution of the Tyr(2) hydroxyl results in the decrease of the agonistic properties of both AVP and OT analogs [75].

In contrast, only in the V1aR and OTR, but not in V2R, one strong interaction occurs, consisting of a salt bridge between the carboxyl of $E^{1.35}$ (– , 54, 42) and Arg(8) guanidinium. In the V2R–AVP complex, Arg(8), considered as mostly involved in the receptor–AVP selectivity [1,7], interacts with the completely different part of the receptor (see the following text).

Nonconserved 7TM and EL2 Residues Control AVP Selectivity

Among the nonconserved 7TM residues that interact with the ligand in V2R, $Q^{4.66}$180 appears to be important for V2R–AVP selectivity. The carboxamide of $Q^{4.66}$180 forms a hydrogen bond with the carboxamide of AVP Asn(5). It is a significant interaction in view of the fact that in the equivalent positions in both V1aR and OTR, the hydrophobic residues (Met and Leu, respectively) occur. Another hydrogen bond can be observed between $R^{5.35}$202 amide proton and the carbonyl of Gly(9). The most important interaction involving EL2 residues that appears exclusively in the V2R–AVP complex is the salt bridge between guanidinium of Arg(8) and carboxyls of D191 and E198 in EL2, simultaneously. In addition, in the V2R–AVP complex, the hydrogen bond between the R181 guanidinium and Asn(5) carboxamide can be observed, while in the V1aR, similar hydrogen bond is formed between R201 and Asn(5) main chain carbonyl. Moreover, in the complex with V1aR, two other hydrogen bonds can be observed, formed between the *C*-terminal carboxamide of AVP and the EL2 N196 carboxamide and T198 main chain carbonyl, simultaneously. However, another strong interaction that might be involved in the V1aR–AVP selectivity is the hydrogen bond between the $T^{7.38}$333 hydroxyl and the carboxamide of the AVP Gln(4). It had been experimentally proved that substitution of Gln(4) significantly reduced binding affinity toward V1aR, but not toward V2R [76,77]. In addition, $T^{7.38}$333 had been proposed as the residue controlling the V_{1a}/V_2 binding selectivity for vasopressin antagonists [78]. For these reasons, the Gln(4)–$T^{7.38}$333 interaction seems to play a key role in binding selectivity for V1aR.

In the OTR–AVP complex, strong and selective interactions as those in the complexes with V2R and V1aR do not occur. Specifically, an important hydrogen bond is formed between the nonconserved $T^{3.40}$127 hydroxyl and the Tyr(2) phenol group. Moreover, there is a possibility of forming a hydrogen bond between two main chain groups in EL2 only: the Gly(9) carbonyl and the EL2 F185 amide proton. Furthermore, the aromatic ring of the latter weakly interacts with the aromatic ring of Phe(3). Remarkably, this EL2 F185 residue was proposed in our earlier work as partially responsible for OTR–OT selectivity [50].

CONCLUSIONS

From the results presented in this study, we consider the highly conserved residues: $Q^{2.57}$, $Q^{2.61}$, $Q^{3.32}$, $Q^{4.60}$, $Q^{6.55}$ as main structural elements stabilizing complexes with AVP, thereby keeping the receptor in the active form in all investigated receptors, analogous to the scheme proposed for complexes with OT [50]. In the majority of stabilizing interactions in which Asn(5) takes part, it might be the crucial handle point in any neurohypophyseal hormone receptor–agonist complex. It has been demonstrated that the substitution of Asn(5) results in the loss of agonistic properties [79]. Moreover, the Gln(4) residue seems to be essential for agonist binding in V1aR in accordance with the experimental data [76,77]. Most of the receptor–AVP interactions

identified in this study are hydrogen bonds or salt bridges, as a result of AVP polarity. Essentially, any hydrophobic interactions significantly affecting ligand binding are not observed, except for a weak EL2 F185–Phe(3) interaction in OTR. In any receptor, there is no strong aromatic stacking interaction with the TM6 aromatic cluster as observed in the complexes of the same receptor with OT antagonists atosiban and barusiban [60,80,81]. It is also in harmony with the experimentally demonstrated fact, that replacement of aromatic TM5 and TM6 residues has no effect on AVP binding in V1aR [78]. Concluding, the lack of strong aromatic agonist–receptor interactions in AVP–receptor complexes might confirm the hypothesis that the TM6 cluster of aromatic residues is involved in stabilization of an inactive state of the receptor as proposed for thyrotropin-releasing hormone (TRH) receptor [82].

In both V2R and V1aR, Arg(8) guanidinium forms strong salt bridges, yet in V2R it interacts with two EL2 acids D191 and E198, whereas in V1aR, it does with $E^{1.35}$(54). These residues located close to extracellular domain might be crucial for AVP recognition, interacting before or during its entry inside the binding pocket. Within the TM domain, the nonconserved residues $Q^{4.66}$180 and $T^{7.38}$333 (in V2R and V1aR, respectively) appear to be most important for the receptor–AVP selectivity. This might suggest a slightly different mechanism of AVP binding to V2R versus V1aR. Consequently, similarity of the interactions identified in the V1aR and OTR (as a salt bridge with $E^{1.35}$) is probably a result of a high-degree sequence identity between these two receptors that is higher than between any of the former and V2R. In fact, the interactions occurring in the OTR–AVP complex were formed during the simulation (docking and MD), but it is obvious that in reality AVP binds to OTR with a small affinity (Table 1).

In summary, the vasopressin receptors are important targets for drug development; therefore identification of residues responsible for AVP binding described in this paper might guide the rational design of both selective agonists and antagonists useful in several pathological conditions.

Acknowledgements

This work is supported by The Polish Scientific Research Committee (KBN), grant no. 3 T09A 11628, The Ministry of Scientific Research and Information Technology (MNiI, Poland) grant no. DS/8372-4-0138-5 and grant for scientific project no. BW/8000-5-0260-5, University of Gdańsk. The computational time in the Academic Computer Center in Gdansk CI TASK, Poland, and the Interdisciplinary Center for Mathematical Modeling (ICM) in Warsaw, Poland, is acknowledged.

REFERENCES

1. Barberis C, Mouillac B, Durroux T. Structural bases of vasopressin/oxytocin receptor function. *J. Endocrinol.* 1998; **156**: 223–229.
2. Zingg HH. Vasopressin and oxytocin receptors. *Baillieres Clin. Endocrinol. Metab.* 1996; **10**: 75–96.
3. Thibonnier M, Berti-Mattera LN, Dulin N, Conarty DM, Mattera R. Signal transduction pathways of the human V1-vascular, V2-renal, V3-pituitary vasopressin and oxytocin receptors. *Prog. Brain Res.* 1998; **119**: 147–161.
4. Peter J, Burbach H, Adan RA, Lolait SJ, Van Leeuwen FW, Mezey E, Palkovits M, Barberis C. Molecular neurobiology and pharmacology of the vasopressin/oxytocin receptor family. *Cell. Mol. Neurobiol.* 1995; **15**: 573–595.
5. Wheatley M, Howl J, Morel A, Davies ARL. Homology between neurohypophysial hormone receptors. *Biochem. J.* 1993; **296**: 519.
6. Hibert M, Hoflack J, Trumpp-Kallmeyer S, Mouillac B, Chini B, Mahe E, Cotte N, Jard S, Manning M, Barberis C. Functional architecture of vasopressin/oxytocin receptors. *J. Recept. Signal Transduct. Res.* 1999; **19**: 589–596.
7. Postina R, Kojro E, Fahrenholz F. Separate agonist and peptide antagonist binding sites of the oxytocin receptor defined by their transfer into the V2 vasopressin receptor. *J. Biol. Chem.* 1996; **271**: 31 593–31 601.
8. Lebl M, Jošt K, Brtník F. Tables of analogs. In *Handbook of Neurohypophysial Hormone Analogs*, Vol. 1, Part 2, Jošt K, Lebl M, Brtník F (eds). CRC Press: Boca Raton, 1987; 127–267.
9. Thibonnier M, Auzan C, Madhun Z, Wilkins P, Berti-Mattera L, Clauser E. Molecular cloning, sequencing, and functional expression of a cDNA encoding the human V1a vasopressin receptor. *J. Biol. Chem.* 1994; **269**: 3304–3310.
10. Howl J, Wheatley M. Molecular pharmacology of V1a vasopressin receptors. *Gen. Pharmacol.* 1995; **26**: 1143–1152.
11. Knepper MA, Valtin H, Sands JM. Renal actions of vasopressin. In *Handbook of physiology*, Vol. III, Oxford University Press, USA: 2000; 496–529.
12. Birnbaumer M, Seibold A, Gilbert S, Ishido M, Barberis C, Antaramian A, Brabet P, Rosenthal W. Molecular cloning of the receptor for human antidiuretic hormone. *Nature* 1992; **357**: 333–335.
13. Sugimoto T, Saito M, Mochizuki S, Watanabe Y, Hashimoto S, Kawashima H. Molecular cloning and functional expression of a cDNA encoding the human V1b vasopressin receptor. *J. Biol. Chem.* 1994; **269**: 27 088–27 092.
14. Thibonnier M, Preston JA, Dulin N, Wilkins PL, Berti-Mattera LN, Mattera R. The human V3 pituitary vasopressin receptor: ligand binding profile and density-dependent signalling pathways. *Endocrinology* 1997; **138**: 4109–4122.
15. Kimura T, Tanizawa O, Mori K, Brownstein MJ, Okayama H. Structure and expression of a human oxytocin receptor. *Nature* 1992; **356**: 526–529.
16. Fuchs AR, Fuchs F, Husslein P, Soloff MS, Fernstrom MJ. Oxytocin receptors and human parturition: a dual role for oxytocin in initiation of labor. *Science* 1982; **215**: 1396–1398.
17. Gimpl G, Fahrenholz F. The oxytocin receptor system: structure, function, and regulation. *Physiol. Rev.* 2001; **81**: 629–683.
18. Barberis C, Tribollet E. Vasopressin and oxytocin receptors in the central nervous system. *Crit. Rev. Neurobiol.* 1996; **10**: 119–154.
19. Corpet F. Multiple sequence alignment with hierarchical clustering. *Nucleic Acids Res.* 1998; **16**: 10 881–10 890.
20. Ballesteros JA, Weinstein H. Integrated methods for modeling G-protein coupled receptors. *Methods Neurosci.* 1995; **25**: 366–428.
21. Palczewski K, Kumasaka T, Hori T, Behnke CA, Motoshima H, Fox BA, Le Trong I, Teller DC, Okada T, Stenkamp RE, Yamamoto M, Miyamoto M. Crystal structure of rhodopsin: a G protein-coupled receptor. *Science* 2000; **289**: 739–745.
22. Lu Z-L, Saldanha JW, Hulme EC. Seven-transmembrane receptors: crystals clarify. *Trends Pharmacol. Sci.* 2002; **23**: 140–146.

23. Ballesteros JA, Shi L, Javitch JA. Structural mimicry in G protein-coupled receptors: implications of the high-resolution structure of rhodopsin for structure-function analysis of rhodopsin-like receptors. *Mol. Pharmacol.* 2001; **60**: 1–19.
24. Sakmar TP. Structure of rhodopsin and the superfamily of seven-helical receptors: the same and not the same. *Curr. Opin. Cell Biol.* 2002; **14**: 189–195.
25. Mirzadegan T, Benko G, Filipek S, Palczewski K. Sequence analyses of G-protein-coupled receptors: similarities to rhodopsin. *Biochemistry* 2003; **42**: 2759–2767.
26. Dowell SJ, Brown AJ. Yeast assays for G-protein-coupled receptors. *Receptors Channels* 2002; **8**: 343–352.
27. Meng EC, Bourne H. Receptor activation: what does the rhodopsin structure tell us?. *Trends Pharmacol. Sci.* 2001; **22**: 587–593.
28. Hunyady L, Vauquelin G, Vanderheyden P. Agonist induction and conformational selection during activation of a G-protein-coupled receptor. *Trends Pharmacol. Sci.* 2003; **24**: 81–86.
29. Bourne HR. How receptors talk to trimeric G proteins. *Curr. Opin. Cell Biol.* 1997; **9**: 134–142.
30. Cabrera-Vera TM, Vanhauwe J, Thomas TO, Medkova M, Preininger A, Mazzoni MR, Hamm HE. Insights into G protein structure, function, and regulation. *Endocr. Rev.* 2003; **24**: 765–781.
31. Sautel M, Milligan G. Molecular manipulation of **G**-protein-coupled receptors: a new avenue into drug discovery. *Curr. Med. Chem.* 2000; **7**: 889–896.
32. Becker OM, Shacham S, Marantz Y, Noiman S. Modeling the 3D structure of GPCRs: advances and application to drug discovery. S. *Curr. Opin. Drug. Discov. Devel.* 2003; **6**: 353–361.
33. Ballesteros J, Palczewski K. G protein-coupled receptor drug discovery: implications from the crystal structure of rhodopsin. *Curr. Opin. Drug Discov. Devel.* 2001; **4**: 561–574.
34. Laszlo FA, Laszlo F Jr, De Wied D. Pharmacology and clinical perspectives of vasopressin antagonists. *Pharmacol. Rev.* 1991; **43**: 73–108.
35. Ziai F, Walter R, Rosenthal IM. Treatment of central diabetes insipidus in adults and children with desmopressin. *Arch. Intern. Med.* 1978; **138**: 1382–1385.
36. Russell SD, DeWald T. Vasopressin receptor antagonists: therapeutic potential in the management of acute and chronic heart failure. *Am. J. Cardiovasc. Drugs* 2003; **3**: 13–20.
37. Mannucci PM. Treatment of von Willebrand's disease. *N. Engl. J. Med.* 2004; **351**: 683–694.
38. Kill C, Wranze E, Wulf H. Successful treatment of severe anaphylactic shock with vasopressin. *Int. Arch. Allergy Immunol.* 2004; **134**: 260–261.
39. Hubbell WL, Altenbach C, Hubbell CM, Khorana HG. Rhodopsin structure, dynamics, and activation: a perspective from crystallography, site-directed spin labeling, sulfhydryl reactivity, and disulfide cross-linking. *Adv. Protein Chem.* 2003; **63**: 243–290.
40. Farrens DL, Altenbach C, Yang K, Hubbell WL, Khorana HG. Requirement of rigid-body motion of transmembrane helices for light activation of rhodopsin. *Science* 1996; **274**: 768–770.
41. Koenig BW. Structure and orientation of ligands bound to membrane proteins are reflected by residual dipolar couplings in solution NMR measurements. *Chembiochem* 2002; **3**: 975–980.
42. Kisselev OG, Kao J, Ponder JW, Fann YC, Gautam N, Marshall GR. Light-activated rhodopsin induces structural binding motif in G protein alpha subunit. *Proc. Natl. Acad. Sci. U.S.A.* 1998; **95**: 4270–4275.
43. Kisselev OG, Downs MA. Rhodopsin controls a conformational switch on the transducin gamma subunit. *Structure* 2003; **11**: 367–373.
44. Hamm HE, Deretic D, Arendt A, Hargrave PA, König B, Hoffman KP. Site of G protein binding to rhodopsin mapped with synthetic peptides from the alpha subunit. *Science* 1988; **241**: 832–835.
45. Martin EL, Rens-Domiano S, Schatz PJ, Hamm HE. Potent peptide analogues of a G protein receptor-binding region obtained with a combinatorial library. *J. Biol. Chem.* 1996; **271**: 361–366.
46. Aris L, Gilchrist A, Rens-Domiano S, Meyer C, Schatz PJ, Dratz EA, Hamm HE. Structural requirements for the stabilization of metarhodopsin II by the C terminus of the alpha subunit of transducin. *J. Biol. Chem.* 2001; **276**: 2333–2339.
47. Janz JM, Farrens DL. Rhodopsin activation exposes a key hydrophobic binding site for the transducin alpha-subunit C terminus. *J. Biol. Chem.* 2004; **279**: 29 767–29 773.
48. Koenig BW, Kontaxis G, Mitchell DC, Louis JM, Litman BJ, Bax A. Structure and orientation of a G protein fragment in the receptor bound state from residual dipolar couplings. *J. Mol. Biol.* 2002; **322**: 441–461.
49. Ślusarz R, Ciarkowski J. Interaction of class A G protein-coupled receptors with G proteins. *Acta Biochim. Pol.* 2004; **51**: 129–136.
50. Ślusarz MJ, Ślusarz R, Ciarkowski J. Molecular dynamics simulation of human neurohypophyseal receptors complexed with oxytocin – modeling of an activated state. *J. Pept. Sci.* in press, DOI:10.1002/psc713.
51. Case DA, Pearlman DA, Caldwell JW, Cheatham TE, Wang J, Ross WS, Simmerling CL, Darden TA, Merz KM, Stanton RV, Cheng A, Vincent JJ, Crowley M, Tsui V, Gohlke H, Radmer R, Duan Y, Pitera J, Massova I, Seibel GL, Singh UC, Weiner P, Kollman PA. *AMBER 7*. University of California: San Francisco, 2002.
52. Cieplak P, Cornell WD, Bayly C, Kollman PA. Application of the multimolecule and multiconformation RESP methodology to biopolymers: charge derivation for DNA, RNA, and proteins. *J. Comput. Chem.* 1995; **16**: 1357–1377.
53. Bayly CI, Cieplak P, Cornell WD, Kollman PA. A well-behaved electrostatic potential based method using charge restraints for deriving atomic charges: the RESP model. *J. Phys. Chem.* 1993; **97**: 10 269–10 280.
54. Schmidt MW, Baldridge KK, Boatz JA, Elbert ST, Gordon MS, Jensen JH, Koseki S, Matsunaga N, Nguyen KA, Su S, Windus TL, Dupuis M, Montgomery JA. The general atomic and molecular electronic structure system. *J. Comput. Chem.* 1993; **14**: 1347–1363.
55. Langs DA, Smith GD, Stezowski JJ, Hughes RE. Structure of pressinoic acid: the cyclic moiety of vasopressin. *Science* 1986; **232**: 1240–1242.
56. *Sybyl® 6.8*. Tripos Inc: St. Louis.
57. Morris GM, Goodsell DS, Halliday RS, Huey R, Hart WE, Belew RK, Olson AJ. Automated docking using a lamarckian genetic algorithm and empirical binding free energy function. *J. Comput. Chem.* 1998; **19**: 1639–1662.
58. Solis FJ, Wets JB. Minimization by random search techniques. *Math. Oper. Res.* 1981; **6**: 19–30.
59. Goodsell DS, Morris GM, Olson AJ. Docking of flexible ligands: applications of AutoDock. *J. Mol. Recognit.* 1996; **9**: 1–5.
60. Ślusarz MJ, Ślusarz R, Kaźmierkiewicz R, Trojnar J, Wioniewski K, Ciarkowski J. Molecular modeling of the neurohypophyseal receptor/atosiban complexes. *Protein Pept. Lett.* 2003; **10**: 295–302.
61. Ślusarz R, Ślusarz MJ, Kaźmierkiewicz R, Lammek B. Molecular modeling of interaction of the vasopressin analogs with vasopressin and oxytocin receptors. *QSAR Comb. Sci.* 2003; **22**: 865–872.
62. Kirkpatrick S, Gelatt CD Jr, Vecchi MP. Optimization by simulated annealing. *Science* 1983; **220**: 671–680.
63. Clore GM, Nilges M, Brünger AT, Karplus M, Gronenborn AM. A comparison of the restrained molecular dynamics and distance geometry methods for determining three-dimensional structures of proteins on the basis of interproton distance restraints. *FEBS Lett.* 1987; **213**: 269–277.
64. Murzyn K, Róg T, Jezierski G, Takaoka Y, Pasenkiewicz-Gierula M. Effects of phospholipid unsaturation on the membrane/water interface: a molecular simulation study. *Biophys. J.* 2001; **81**: 170–183.
65. Pasenkiewicz-Gierula M, Murzyn K, Róg T, Czaplewski C. Molecular dynamics simulation studies of lipid bilayer systems. *Acta Biochim. Pol.* 2000; **47**: 601–611.

66. Ewald PP. Die Berechnung optischer und elektrostatischer Gitterpotentiale. *Ann. Phys.* 1921; **64**: 253–287.
67. Darden T, York D, Petersen L. Partial mesh Ewald: an N x log(N) method for Ewalds sums in large systems. *J. Chem. Phys.* 1993; **98**: 10 089–10 092.
68. Essmann UL, Perera ML, Berkowitz T, Darden T, Lee H, Pedersen LG. A smooth particle mesh Ewald method. *J. Chem. Phys.* 1995; **103**: 8577–8593.
69. Jorgensen WL, Tirado-Rives J. The OPLS potential functions for proteins. Energy minimization for crystals of cyclic peptides and crambin. *J. Am. Chem. Soc.* 1988; **110**: 1657–1666.
70. Walter R. Identification of sites in oxytocin involved in uterine receptor recognition and activation. *Fed. Proc. Am. Soc. Exp. Biol.* 1977; **36**: 1872–1878.
71. Wood SP, Tickle IJ, Treharne AM, Pitts JE, Mascarenhas Y, Li JY, Husain J, Cooper S, Blundell TL, Hruby VJ, Wyssbrod HR, Buku A, Fishman AJ. Crystal structure analysis of deamino-oxytocin: conformational flexibility and receptor binding. *Science* 1986; **232**: 633–636.
72. Manning M, Bankowski K, Sawyer WH. Selective agonists and antagonists of vasopressin. In *Vasopressin*, Gash DW, Boer GJ (eds). Plenum Publishing: New York, 1987; 335–368.
73. Sawyer WH, Grzonka Z, Manning M. Neurohypophyseal peptides. Design of tissue-specific agonists and antagonists. *Mol. Cell. Endocrinol.* 1981; **22**: 117–134.
74. Mouillac B, Chini B, Balestre MN, Elands J, Trumpp KS, Hoflack J, Hibert M, Jard S, Barberis C. The binding site of neuropeptide vasopressin V1a receptor. Evidence for a major localization within transmembrane regions. *J. Biol. Chem.* 1995; **270**: 25 771–25 777.
75. Manning M, Sawyer WH. The development of selective agonists and antagonists of vasopressin. In *Vasopressin*, Schrier RW (ed.). Raven Press: New York, 1985; 131–144.
76. Sawyer WH, Acosta M, Balaspiri L, Judd J, Manning M. Structural changes in the arginine vasopressin molecule that enhance antidiuretic activity and specificity. *Endocrinology* 1974; **94**: 1106–1115.
77. Gillessen D, du Vigneaud V. The synthesis and pharmacological properties of 4-decarboxamide-8-1ysinevasopressin, 5-decarboxamide-8-1ysinevasopressin, and their l-deamino analogs. *J. Biol. Chem.* 1967; **242**: 4806–4812.
78. Cotte N, Balestre MN, Aumelas A, Mahé E, Phalipou S, Morin D, Hibert M, Manning M, Durroux T, Barberis C, Mouillac B. Conserved aromatic residues in the transmembrane region VI of the V1a vasopressin receptor differentiate agonist vs. antagonist ligand binding. *Eur. J. Biochem.* 2000; **267**: 4253–4263.
79. Chan WY, Wo NC, Cheng LL, Manning M. Isosteric substitution of Asn5 in antagonists of oxytocin and vasopressin leads to highly selective and potent oxytocin and V1a receptor antagonists: new approaches for the design of potential tocolytics for preterm labor. *J. Pharmacol. Exp. Ther.* 1996; **277**: 999–1003.
80. Ślusarz MJ, Ślusarz R, Meadows R, Trojnar J, Ciarkowski J. Molecular dynamics of complexes of atosiban with neurohypophyseal receptors in the fully hydrated phospolipid bilayer. *QSAR Comb. Sci.* 2004; **23**: 536–545.
81. Ślusarz MJ, Giełdoń A, Ślusarz R, Meadows R, Trojnar J, Ciarkowski J. Study of new oxytocin antagonist barusiban (Fe200 440) affinity toward human oxytocin receptor versus vasopressin V1a and V2 receptors – molecular dynamics simulation in POPC bilayer. *QSAR Comb. Sci.* 2005; **24**: 603–610.
82. Colson AO, Perlman JH, Jinsi-Parimoo A, Nussenzveig DR, Osman R, Gershengorn MC. A hydrophobic cluster between transmembrane helices 5 ~and 6 ~Constrains the thyrotropin-releasing hormone receptor in an inactive conformation. *Mol. Pharmacol.* 1998; **54**: 968–978.